Fragmentation statistics of large H_2O and NH_3 clusters from molecular-dynamics simulations

T. A. Beu*
Faculty of Physics, University "Babeş-Bolyai," RO-3400 Cluj-Napoca, Romania
(Received 6 December 2002; published 25 April 2003)

The fragmentation statistics of $(H_2O)_N$ and $(NH_3)_N$ clusters ($N=100-1000$) is investigated by molecular-dynamics simulations. The fragment size distributions are found to be well described by power laws over a wide range of excitation energies. The maximum fragment size depends linearly on the cluster size. A compact analytical model, implying the maximum fragment size and the power-law exponent of the fragment size distribution, is shown to fit the average fragment size profiles quite well. It is demonstrated that the proposed relationship can be used to predict reliable fragment size distributions, starting from fits of the maximum and the average fragment sizes.

DOI: 10.1103/PhysRevA.67.045201 PACS number(s): 36.40.Qv

Fragmentation is a very appealing investigation topic for at least the following reasons: first, the omnipresence of fragmentation processes in nature, on very different space and time scales; second, the rather particular character of the systems investigated so far; third, the still open issue regarding the hypothetical existence of a universal mechanism governing fragmentation.

For the class of percolation clusters in particular, intensive theoretical studies have been done, mainly based on the scaling ansatz $P_N(s)\sim s^{-\phi}G(s/N)$ for the formation probability of a fragment of size s from a cluster of size N [1–4]. Edwards *et al.* [1] applied simulations and exact enumeration to investigate this scaling law for bond percolation clusters, while Debierre [2] deduced from large-scale simulations the exact fragmentation exponent $\phi=1.548$. Campi *et al.* [3] reported fragment size distributions from high-energy nuclear collisions, which are also remarkably well reproduced by a percolation model, too. Gross *et al.* [5] studied the fragmentation phase transition in atomic clusters.

Topics regarding the energy redistribution and fragmentation behavior of large water clusters, in particular, have been addressed by Svanberg *et al.* [6] in their molecular-dynamics (MD) study on the collision dynamics of large water clusters. Fragmentation experiments on large ammonia and water clusters using electron impact ionization have been reported by Bobbert *et al.* [7].

The primary objective of the present work was to investigate the fragmentation statistics of large water and ammonia clusters by molecular dynamics, on the basis of a realistic site-site intermolecular potential. To achieve this goal, essentially (a) equilibrium geometrical structures and (b) fragment size distributions have been calculated.

Both the H_2O and NH_3 monomers were considered to be rigid. The interactions of the H_2O molecule were modeled by the TIP4P transferable intermolecular potential function (with four interaction sites) of Jorgensen *et al.* [8], intensively used in the last two decades in simulations of aqueous solutions and clusters. For the NH_3 molecule, the five-site potential of Impey and Klein [9] was employed, which has proved successful in simulations of liquid ammonia and of structural and spectroscopic properties of clusters [10].

The MD integrator employed was the Verlet algorithm in the quaternion representation, known to have fair energy conservation properties. We have used throughout a time step of 0.2 fs, typically ensuring a relative energy conservation error of less than 10^{-4}.

For both molecular species, clusters of sizes $N=100-1000$, with an increment of 100 molecules, were prepared by simulated annealing. For the temperature, the usual definition, as the mean kinetic energy per degree of freedom, was adopted. The initial configuration of each cluster was chosen to be a sphere cut from the respective crystal (cubic ice for water [11]; for crystalline ammonia see [12]). After an initial uniform heating at 150 K (by assigning random, properly normalized velocities to all molecules), the crystal spheres were cooled off for 100 ps, by removing 1% of the kinetic energy at each time step. For each cluster size, the energetically lowest of 10 different relaxed configurations was adopted as the equilibrium structure.

The equilibrium configurations for the water clusters with $N=100$ and 1000 are depicted in Fig. 1. It can be noticed that the original crystalline arrangement is preserved to an extent increasing with the cluster size, the weight of the amorphous outer shell decreasing concomitantly. The qualitative behavior of the NH_3 clusters is absolutely similar.

The size dependence of the binding energies of the equilibrium structures found is characterized by the almost constant values $E_{\mathrm{bind}}/N=46.55$ kJ/mol for the water clusters and $E_{\mathrm{bind}}/N=29.51$ kJ/mol for the ammonia clusters. The maximal extent and the gyration radius of the H_2O clusters can be very accurately represented by the fits $R_{\max}$

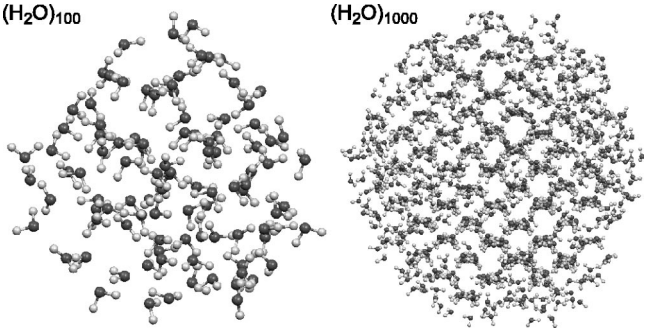

FIG. 1. Geometrical equilibrium structures of the clusters $(H_2O)_{100}$ and $(H_2O)_{1000}$.

*Electronic address: tbeu@phys.ubbcluj.ro

$=2.762N^{0.3986}$ and $R_{\mathrm{gyr}}=1.245N^{0.3595}$, respectively, with exponents quite close to the intuitive value of 1/3. The dependences in the case of the NH_3 clusters are $R_{\max}=3.876N^{0.3336}$ and $R_{\mathrm{gyr}}=1.508N^{0.3330}$.

In order to characterize the extent to which the cluster structures preserve the initial crystalline arrangement, we defined the ''crystallinity''

$$\chi=\sum_i \langle \mathbf{r}_i\cdot\mathbf{r}_i^c\rangle/\sum_i \langle \mathbf{r}_i^c\cdot\mathbf{r}_i^c\rangle$$

as the normalized projection of the final atomic positions $\mathbf{r}_i$ onto the corresponding crystalline positions $\mathbf{r}_i^c$. The calculated crystallinity values suggest the cluster size dependence

$$\chi=1-aN^{-b}$$

and the regression yields $a=1.662$ and $b=0.572$ for H_2O. However, a quite reasonable fit results also by using the single-parameter functional with $b=2/3$ (intuitively, the crystallinity should increase toward 1 by a quantity inversely proportional to the surface-to-volume ratio). The optimized parameter for H_2O in this case is $a=2.761$.

The excitation mechanism leading to fragmentation was chosen of extreme simplicity, avoiding artifacts which might have arisen from particular excitations and thus preserving the generality of the results. Concretely, all molecules acquire initially random velocities, normalized according to the temperature.

The excitation temperatures considered for H_2O were $T=1500$, 1650, 2000, 2500, and 3000 K, corresponding to total excitation energies between $0.8E_{\mathrm{bind}}$ and $1.6E_{\mathrm{bind}}$ (E_{bind} being the binding energy of the cluster). Since, statistically, the H_2O clusters survive unfragmented below this temperature range, lower temperatures were not considered. For similar reasons, the NH_3 clusters were heated to $T=1000$, 1100, 1200, 1300, and 1500 K, corresponding to total excitation energies between $0.8E_{\mathrm{bind}}$ and $1.3E_{\mathrm{bind}}$.

Each fragmentation trajectory was propagated at constant energy for about 10 ps, until the overall extent of the fragment cloud exceeded four times the initial extent. At the end of the trajectory, the individual fragments were identified by a recursive labeling algorithm, which basically extends the fragments gradually by molecules which lie within a cutoff distance. The cutoff was defined as the minimum intermolecular distance in the relaxed cluster increased by 1 Å.

In order to achieve reliable statistics, an ensemble of 50 identical clusters was fragmented for each molecular species, excitation temperature, and cluster size, and the resulting profiles were averaged. Thus, the fragment size distribution $P_N(s)$ specifies the average number of fragments of each particular size s resulting from the cluster of size N, and is normalized such that $\Sigma_s sP_N(s)=1$.

Several general findings may be obtained by inspecting the typical fragmentation profiles presented in Fig. 2 for the relaxed $(H_2O)_{1000}$ and $(NH_3)_{1000}$ clusters. First, the profiles for larger excitation temperatures imply relatively more small fragments at the expense of the larger ones, reflecting the fact that larger energy inputs split the original cluster into

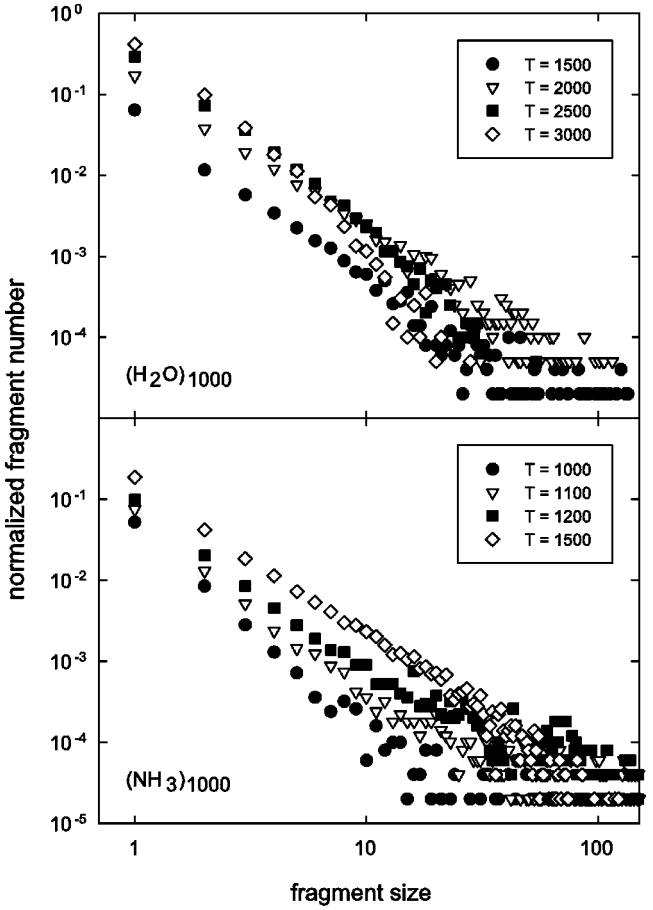

FIG. 2. Fragment size distributions for the $(H_2O)_{1000}$ and $(NH_3)_{1000}$ clusters.

smaller fragments. Second, all profiles are affected by statistical fluctuations in the region of larger and inherently less frequent fragment sizes. Third, in the lower-temperature region, the profiles for both molecular species clearly exhibit power-law behavior,

$$P_N(s)\sim s^{-\phi_N}, \tag{1}$$

similar to the thoroughly investigated percolation clusters [2]. The overall features of the fragmentation profiles are similar to those found in the distributions obtained by Svanberg *et al.* [6] from simulations of the collision dynamics of large water clusters.

The fragmentation of the H_2O clusters above 2500 K ($E_{\mathrm{exc}}\geqslant 1.3E_{\mathrm{bind}}$) seems to be somewhat better described by stretched exponentials. In the case of NH_3, the transition to stretched exponentials occurs at 1500 K (i.e., again for $E_{\mathrm{exc}}\geqslant 1.3E_{\mathrm{bind}}$).

The maximum fragment sizes $s_{\max,N}$ featured by the calculated distributions appear to vary linearly with the cluster size and the slopes decrease with increasing temperature. The profiles for the water clusters are plotted in Fig. 3. Indeed, the plots are expected to be delimited by the first bisector, $s_{\max,N}=N$, corresponding to the limiting case $T=0$ (where no fragmentation takes place), and the horizontal line $s_{\max,N}=1$, corresponding to $T\to\infty$ (when all clusters are

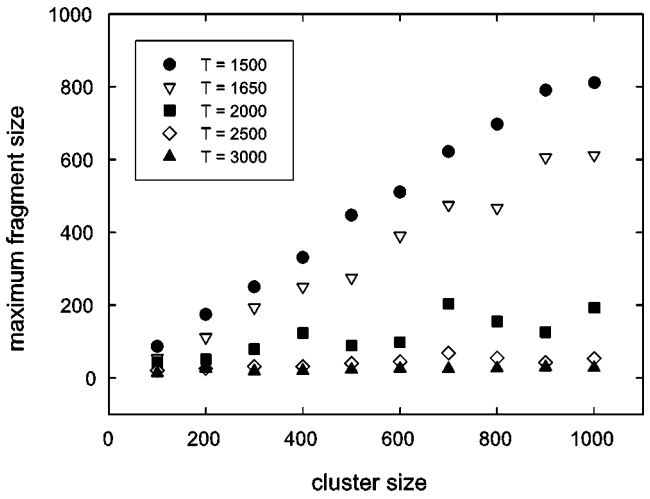

FIG. 3. Maximum fragment size as a function of the size of the original $(H_2O)_N$ cluster.

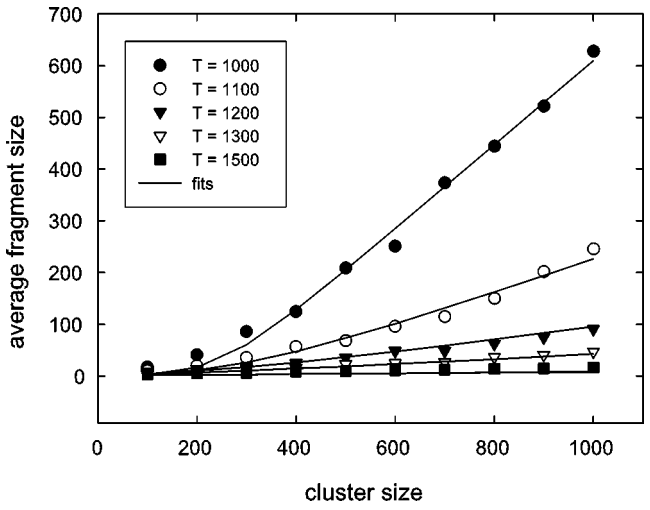

FIG. 4. Average fragment size as a function of the size of the original $(NH_3)_N$ cluster and fit curves (see text).

completely fragmented down to monomers). The dependence of the maximum fragment size on the cluster size can thus be represented as

$$s_{\max,N}=1+a(N-1). \tag{2}$$

The values obtained by regression for the parameter a suggest that its dependence on the excitation temperature is a simple exponential decay:

$$a(T)=a_1\exp(-a_2T). \tag{3}$$

The temperature fits yield $a_1=33.5827$ and $a_2=2.4472\times10^{-3}$ K^{-1} for the water clusters, while for the ammonia clusters $a_1=3298.27$ and $a_2=7.8352\times10^{-3}$ K^{-1}.

The only available size-resolved experimental data stem from the fragmentation experiments by electron impact on water and ammonia clusters reported by Bobbert *et al.* [7]. Figure 6 of their paper presents the linear dependence of the number of evaporated molecules on the initial cluster size. By subtracting the reported figures from the corresponding cluster sizes, one obtains just the measured maximum (residual) fragment sizes. Their dependence on the initial cluster size is linear, in qualitative agreement with our model, even though the excitation mechanisms are quite different.

The cluster size dependences of the average fragment size $\langle s\rangle_N$ for the various excitation temperatures are shown in Fig. 4 for the NH_3 clusters. Absolutely similar dependences are obtained for the H_2O clusters. The profiles are again delimited by the lines $\langle s\rangle_N=N$ and $\langle s\rangle_N=1$ for the same reasons as in the case of $s_{\max,N}$. By definition, the average fragment size is given by

$$\langle s\rangle_N=\frac{\sum_{s=1}^{s_{\max,N}} s^2P_N(s)}{\sum_{s=1}^{s_{\max,N}} sP_N(s)}.$$

An approximate analytic expression may be readily obtained by replacing the sums by integrals ($\Sigma_{s=1}^{s_{\max,N}}\cdots\simeq\int_1^{s_{\max,N}}\cdots ds$) and by using the power-law distribution (1):

$$\langle s\rangle_N=\frac{2-\phi_N}{3-\phi_N}\frac{s_{\max,N}^{3-\phi_N}-1}{s_{\max,N}^{2-\phi_N}-1}. \tag{4}$$

For known values of the power-law exponent ϕ_N and of the maximum fragment size $s_{\max,N}$, this relation should provide consistently an estimate of the average fragment size $\langle s\rangle_N$. For practical applications, however, this is hardly the case. Whereas measurements are likely to provide $s_{\max,N}$ and $\langle s\rangle_N$, the fragment size distribution itself is more difficult to obtain. Instead, relation (4) can be used in conjunction with the N dependence of $s_{\max,N}$ [Eq. (2)] to deconvolve the fragmentation information obtaining ϕ_N, and thus to predict the fragment size distribution.

The plots of the power-law exponent ϕ_N (shown in Fig. 5 for the NH_3 clusters) suggest a simple power-law dependence on the cluster size:

$$\phi_N=bN^{-c}. \tag{5}$$

Relations (2), (4), and (5) define explicitly the average fragment size $\langle s\rangle_N$ as a function of the cluster size N, with adjustable parameters b and c. This set of equations was used to simultaneously fit the cluster size dependences of the average fragment size and of the power-law exponents. The optimized values of the parameters b and c for the various temperatures suggest the exponential dependences

$$b(T)=b_0+b_1\exp(-b_2T), \tag{6}$$

$$c(T)=c_1\exp(-c_2T). \tag{7}$$

The actual fit yields for the H_2O clusters $b_0=3.1976$, $b_1=494.22$, $b_2=3.1308\times10^{-3}$ K^{-1}, $c_1=9.3408$, and $c_2=2.2969\times10^{-3}$ K^{-1}. The values for the NH_3 clusters are

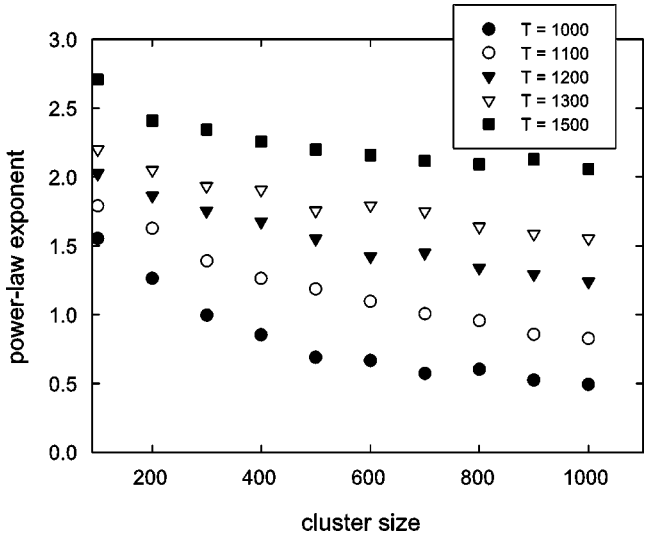

FIG. 5. Dependence of the power-law exponents of the fragment size distributions on the size of the initial $(NH_3)_N$ clusters.

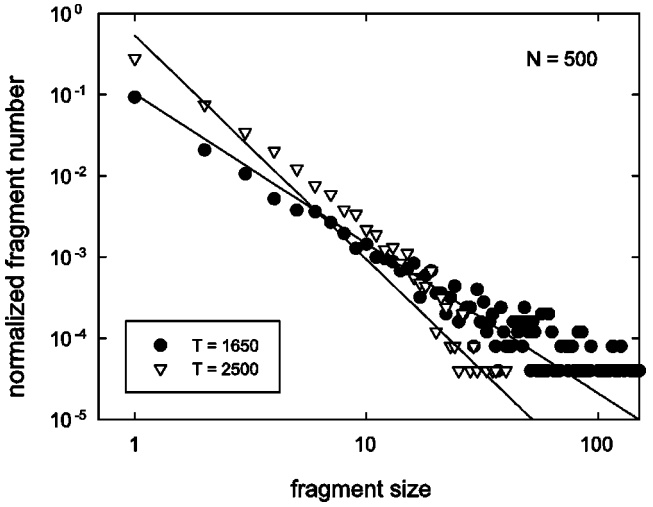

FIG. 6. Simulated fragment size distributions and profiles resulted from model (2)–(7) for the $(H_2O)_{500}$ cluster heated at $T=1650$ K and $T=2000$ K, respectively.

$b_0=3.1895$, $b_1=233\,574$, $b_2=8.9334\times10^{-3}\ \mathrm{K}^{-1}$, $c_1=15.3306$, and $c_2=3.4363\times10^{-3}\ \mathrm{K}^{-1}$.

The appropriateness of model (4) and the quality of the presented multidimensional fits can be judged from the typical results shown in Fig. 6. Here, along with the simulated fragment size distributions for the cluster $(H_2O)_{500}$ heated at $T=1650$ K and $T=2500$ K, respectively, there have been plotted the corresponding curves resulting by using the model (2), (4), and (5), together with the temperature fits of the implied parameters $a(T)$, $b(T)$, and $c(T)$. It is worth reemphasizing that the continuous lines *are not* direct fits of the simulated fragment sizes. Equally good agreement is found between the simulated fragmentation profiles and the proposed model in the case of the ammonia clusters.

The slight discrepancies between model and observations occurring in the low-temperature region are due to the inherently more significant fluctuations. To overcome these, larger ensembles of observations are needed. The discrepancies at large excitation energies (beyond $1.3E_{\mathrm{bind}}$) are caused by the gradual transition of the profiles into stretched exponentials. However, the fair overall agreement validates the model and justifies its applicability for extracting the exponents of the fragment size distribution from maximum and average fragment sizes.

In conclusion, the fragment size distributions are found to be well described by power laws for excitation energies up to $1.3E_{\mathrm{bind}}$ and by stretched exponentials at larger excitation energies. The power-law exponents show power-law dependence on the cluster size themselves, while the maximum fragment size depends linearly on the cluster size. A simple analytical model, implying the maximum fragment size and the power-law exponent of the fragment size distribution, fits the average fragment size profiles quite well. The proposed model can be used conversely to predict reliable fragment size distributions starting from fits of the maximum and average fragment sizes. The dependence of the model parameters on the excitation temperature (energy) is given solely by exponential decays.

This work was supported by the Alexander-von-Humboldt-Stiftung. Special thanks go to Professor Udo Buck for the stimulating discussions and the hospitality at the Max-Planck-Institut für Strömungsforschung from Göttingen.

[1] B. F. Edwards, M. F. Gyure, and M. Ferer, Phys. Rev. A **46**, 6252 (1992).
[2] J.-M. Debierre, Phys. Rev. Lett. **78**, 3145 (1997).
[3] X. Campi, H. Krivine, N. Sator, and E. Plagnol, Eur. Phys. J. D **11**, 233 (2000).
[4] X. Campi, H. Krivine, and N. Sator, Physica A **296**, 24 (2001).
[5] D. H. E. Gross, M. E. Madjet, and O. Schapiro, Z. Phys. D: At., Mol. Clusters **39**, 75 (1997).
[6] M. Svanberg, L. Ming, N. Markovic, and J. B. C. Petterson, J. Chem. Phys. **108**, 5888 (1998).
[7] C. Bobbert, S. Schiitte, C. Steinbach, and U. Buck, Eur. Phys. J. D **19**, 183 (2002).
[8] W. L. Jorgensen, J. Chandrasekhar, J. D. Madura, R. W. Impey, and M. L. Klein, J. Chem. Phys. **79**, 926 (1983).
[9] R. W. Impey and M. L. Klein, Chem. Phys. Lett. **104**, 579 (1984).
[10] T. A. Beu, C. Steinbach, and U. Buck, J. Chem. Phys. **117**, 3149 (2002).
[11] L. G. Dowell and A. P. Rinfret, Nature (London) **188**, 1144 (1960).
[12] J. W. Reed and P. M. Harris, J. Chem. Phys. **35**, 1730 (1961).